Acoustic streaming in two-dimensional freely suspended smectic liquid crystal films

S. V. Yablonskii,[1,2] N. M. Kurbatov,[2,3] and V. M. Parfenyev[1,*]

[1]*Landau Institute for Theoretical Physics of the Russian Academy of Sciences, 142432 Akademica Semenova av. 1-A, Chernogolovka, Russia*

[2]*Shubnikov Institute of Crystallography of Federal Scientific Research Center "Crystallography and Photonics" of the Russian Academy of Sciences, 119333 Leninsky pr. 59, Moscow, Russia*

[3]*Moscow Institute of Physics and Technology, 141700 Institutskiy per. 9, Dolgoprudny, Russia*

(Received 1 November 2016; revised manuscript received 19 December 2016; published 24 January 2017)

We study horizontal streaming excited by means of a low-frequency and low-intensity acoustic wave in 2D freely suspended films of thermotropic smectic liquid crystals. Acoustic pressure induces fast periodic transverse oscillations of the film, which produce in-plane stationary couples of vortices slowly rotating in opposite directions owing to hydrodynamic nonlinearity. The parameters of the vortices are measured using a new method, based on tracking solidlike disk-shaped islands. The horizontal motion occurs only when the amplitude of the acoustic pressure exceeds the threshold value, which can be explained by Bingham-like behavior of the smectic film. The measurements above threshold are in good agreement with existing theoretical predictions. We demonstrate experimentally that in-plane flow is well controlled by changing the acoustic pressure, excitation frequency, and geometry of the film. The observations open the way to using the phenomenon in nondisplay applications.

DOI: 10.1103/PhysRevE.95.012707

Introduction. Discovered by Otto Lehmann and Friedrich Reinitzer more than 100 years ago, thermotropic liquid crystals are used everywhere [1]. Lyotropic liquid crystals, substances similar to ordinary soap combined with water, were known much earlier and their importance in everyday life is also not in doubt [2]. The main application of thermotropic liquid crystals is the production of displays [3]. Other applications (so-called "nondisplay" field) include, e.g., the development of panels with controllable light transmission [4] and the visualization of thermal fields in medicine and aeronautics [5]. Thermotropic smectic liquid crystals possess a microscopic layered structure that promotes the formation of a macroscopic steady state in the form of a uniform-thickness, freely suspended film without contact with bearing surfaces [6]. The bending motion of such films is well studied and its properties allow the use of smectic films as sensitive elements in detectors of visible and IR radiation [7].

In this paper, we investigate experimentally acoustically stimulated horizontal streaming in freely suspended smectic films, which was predicted recently [8], and discuss possible applications of the phenomenon. The earliest example of acoustic streaming refers to vortex spots in soap films [9], and it is close to experiments discussed below. An important and fundamental difference between the acoustic streaming in thermotropic smectic films and that in soap films is the lack of tangential stresses associated with the Marangoni effect [10] in the first case. Here, acoustic streaming originated in the constant-thickness membrane composed of individual mesogenic substance. The in-plane motion has the form of stationary vortices rotating in opposite directions, which can be controlled by the parameters of the acoustic wave and geometry of the film.

Qualitatively, the appearance of vortices can be understood as follows. The acoustic wave excites transverse oscillations of the film, which involve surrounding air in motion. The motion of air can be characterized by the velocity field $\boldsymbol{v}$, which obeys the Navier-Stokes equation. Mainly, this motion is potential and therefore it cannot generate vortices, but the kinematic viscosity of air ν_a violates this approximation. It turns out that in the linear regime the air motion has nonzero horizontal vorticity, $\varpi_\alpha = [\mathrm{rot}\,\boldsymbol{v}]_\alpha$, $\alpha = \{x, y\}$, concentrated in a thin viscous sublayer near the film surface. The vertical vorticity ϖ_z is 0 in this approximation; it appears only due to second-order nonlinear interaction. From the Navier-Stokes equation one can obtain the equation for the vertical vorticity ϖ_z [8]:

$$\partial_t \varpi_z + (\boldsymbol{v}\nabla)\varpi_z - \nu_a \nabla^2 \varpi_z = \varpi_\alpha \partial_\alpha v_z. \tag{1}$$

The term on the right-hand side can be regarded as a source with respect to ϖ_z. It corresponds to the rotation of the horizontal vorticity ϖ_α by the vertical velocity v_z [see Fig. 1(a)]. As a result, we obtain the vertical vorticity—the vortices in the film plane [see Fig. 1(b)]. The quantitative theory of this phenomenon was developed in Ref. [8]. We also would like to note that a similar mechanism generates horizontal vortices on the surface of a liquid [11].

The vortex flow is analyzed by observing the motion of disk-shaped solidlike islands generated on the film surface in a special way [12] [see Fig. 1(b)]. We demonstrate that the horizontal streaming occurs only if the amplitude of the acoustic pressure exceeds a certain value. The vortex motion arises abruptly; the velocity of islands shows a discontinuity at threshold. Above threshold the amplitude of the streaming is proportional to the squared acoustic pressure in accordance with existing theory [8]. We discuss the threshold behavior and speculate that it can be explained by a Bingham-like mechanism [13]. Experimental data also show that 2D freely suspended smectic films are sufficiently robust and can withstand moderate levels of mechanical shock without degradation of their characteristics. This allows their use in nondisplay applications, which are discussed later in the paper.

*parfenius@gmail.com

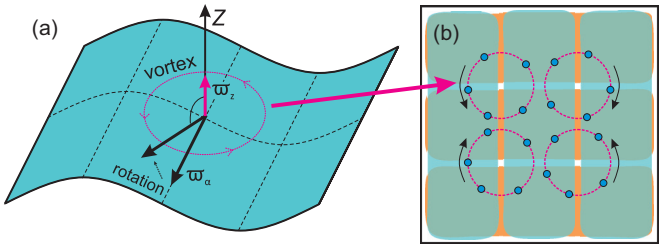

FIG. 1. (a) The horizontal vorticity ϖ_α, which arises due to the air viscosity, is slightly rotated by the surface tilt. As a result, this nonlinear interaction produces the vertical vorticity ϖ_z—vortices in the film plane; (b) vortices in the film plane visualized by disk-shaped islands. This vortex flow corresponds to the excitation of (3,1) and (1,3) bending modes slightly time-shifted relative to each other.

Methods. A freely suspended smectic film was prepared by manipulation with mobile barriers [6] as shown in Fig. 2(a), (1–3). A drop of liquid crystal was placed in a narrow gap between two barriers, which then were slowly moved to a predetermined size. During experiments, the barriers can be shifted relative to each other changing the aspect ratio of the rectangular film. The distance between guide rails was fixed at $a = 16.5$ mm and the distance between mobile barriers b ranged from 0 to 60 mm. The thickness of the freely suspended smectic film was determined by the color in reflected white light, as was done by Sirota *et al.* [14]. The film color was blue, corresponding to the number of layers $N = 62 \pm 5$ and film thickness $h = Nd \approx 200$ nm, where each smectic layer has a thickness $d = 3.17$ nm [15]. By selecting a certain initial amount of the liquid crystal we always managed to obtain a film of uniform thickness with acceptable accuracy. Additional confirmation of the film thickness was performed by fitting the theoretical reflection spectrum and the reflection spectrum obtained by the CCD AvaSpec-ULS2048 spectrometer [6]. The measurements were performed with the liquid crystal *n*-octyl-cyano-biphenyl 8CB, which exhibits a S_A phase between 21.0° and 33.0° C. The purity of 8CB (NIOPIK) was 99%. The working temperatures were 22°–28° C.

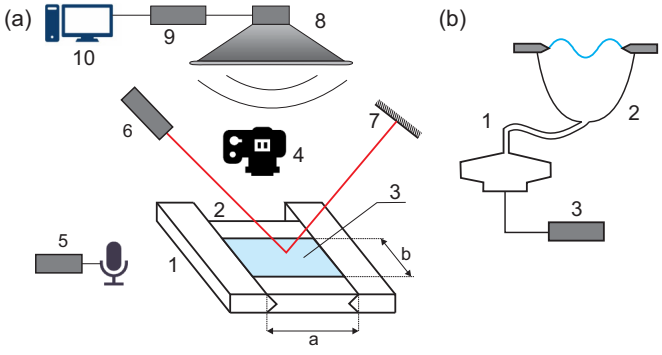

FIG. 2. (a) Experimental setup for the study of vibration and vortex motion in the liquid crystal membrane: 1, guide rails; 2, mobile barriers; 3, liquid crystal membrane; 4, digital camera; 5, condenser microphone connected to the acoustic power meter; 6, laser; 7, screen; 8, loudspeaker; 9, low-frequency generator based on the PC sound card; 10, computer. (b) Acoustic excitation by the waveguide: 1, sound waveguide; 2, frame with the membrane; 3, sound generator.

Transverse vibrations of the smectic film and the vortex flow were excited by an electrodynamic loudspeaker, (8), acting as a piston [see Fig. 2(a)]. A frame with the film was placed in the far field, which was uniform, with an accuracy of 3% on the acoustic pressure amplitude. The frequency and amplitude of the acoustic wave were controlled by computer, (10). The acoustic pressure was measured by a condenser microphone connected to a Robotron-017 sound-level meter, (5). In the experiments we varied the size of the membrane b, the excitation frequency ν, and the amplitude of the acoustic pressure Δp. The thickness of the film with an acceptable accuracy was constant. We also investigated the horizontal streaming excited by a strongly inhomogeneous acoustic field formed by means of an acoustic waveguide, as shown in Fig. 2(b). In this case, the amplitude of the acoustic heterogeneity on the surface of the membrane reached 25%. This method of excitation allows us to obtain more intense streaming, but the transverse vibrations of the membrane are rather complex and cannot be well controlled.

To study the horizontal flow in the smectic film we tried various known methods of adding passive particles to the film surface. By monitoring the motion of these particles it is possible to restore the velocity field in the film plane [16]. Attempts were made to use micron-sized polystyrene beads, but either the film was destroyed or particles were collected on the periphery of the film in the region of the meniscus. The known method of creating colored liquid for monitoring flow using photochromic labels [17] was also ineffective, because the film thickness is too small and therefore one cannot reach the necessary contrast. Eventually, we found a convenient way to visualize the flow by observing the motion of disk-shaped islands generated on the film surface [see Fig. 1(b)]. To generate these islands mobile barriers, (2), were abruptly shrunk by about 1–2 mm [see Fig. 2(a)]. The procedure allows us to get a controllably different number of long-lived islands, whose sizes are in the range of 0.01 to 0.5 mm.

At a high acoustic pressure (more than ~0.16 Pa for the parameters used; see below) these islands cannot be treated as passive tracers. For example, they were gathered together on the same current line regardless of their formation place (see Fig. 3(a) and Ref. [18(1)]). However, at a lower acoustic pressure, they manifest Lagrangian particle behavior quite well, and their motion provides information on the in-plane flow in the bed of standard theory. The transition between

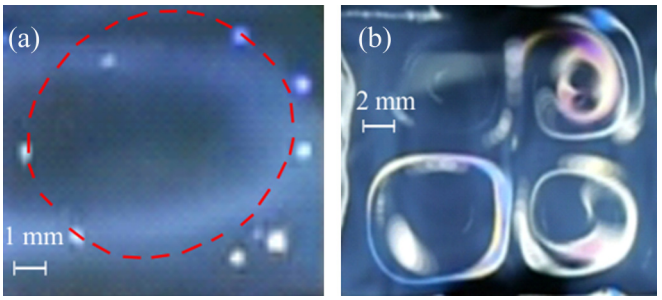

FIG. 3. Horizontal streaming at a high acoustic pressure: (a) Vortex visualized by disk-shaped islands. The dotted line shows the trajectory of islands. (b) Four vortices visualized by an excess number of islands.

two regimes is shown in video [18(2)]. The advantage of the proposed observation method can be seen with the naked eye (compare Fig. 3(a) vs Fig. 3(b) and Ref. [18(1)] vs Ref. [18(3)]. The last ones show a vortex motion in the case of visualization by a large number of islands and high acoustic pressure. Photos similar in quality were obtained earlier in experiments with soap films [19].

Results. Stationary vortex flow is generated due to nonlinear interaction of bending modes excited in the film [8]. Therefore, acoustic streaming occurs near the frequencies corresponding to the resonance conditions of smectic film transverse oscillations,

$$\nu_{nm} = \frac{|k_{nm}|}{2\pi}\sqrt{\frac{2\sigma}{\rho_s}}, \quad \rho_s = \rho_{\mathrm{LC}}h + 2\rho_a/|k_{nm}|, \qquad (2)$$

where $|k_{nm}| = \pi\sqrt{(n/a)^2 + (m/b)^2}$ is the wave number of the bending mode, $\sigma = 29.2$ dyn/cm is the surface tension of the liquid crystal 8CB, and ρ_s is the surface density of the film including the mass of air involved in motion. The volume densities of liquid crystal 8CB and air are equal to $\rho_{\mathrm{LC}} = 0.96$ g/cm^3 and $\rho_a(25^\circ\,\mathrm{C}) = 1.2 \times 10^{-3}$ g/cm^3, respectively. The plane acoustic wave effectively excites only modes (n,m) with odd indices [6]. The other essential point in the experimental observation of coherent vortex structures is the small "detuning" in the geometry of the film; it should be nearly square to produce a time shift between excited bending modes [8]. We address this question in detail in the next section.

Further, we consider such a film, $a = 16.5$ mm and $b = 17$ mm, where bending modes (3,1) and (1,3) are excited. The selection of these particular modes is caused by the following reason. They have odd indices and so they can be excited effectively by a plane acoustic wave. They also have different indices, $n \neq m$, and therefore their eigenfrequencies differ slightly, which produces the necessary time-shift between them. Using Eq. (2) one finds the resonance frequencies of these modes, $\nu_{31} = 357$ Hz and $\nu_{13} = 344$ Hz. Note that the mass of air involved in motion is much larger than the mass of the smectic film, i.e., $2\rho_a/\rho_{\mathrm{LC}}hk \approx 20$.

Experimentally, the resonance frequency close to 350 Hz was recorded [see Fig. 4(a)]. It was obtained by measuring the size of the laser beam projection on a screen after reflection from a surface of the film vs the frequency of the acoustic excitation [see Fig. 2(a), (6 and 7)]. The Q factors of resonances (3,1) and (1,3) are not very high and they merge into a single curve. The indices of excited modes were verified by examining optical images of the laser beam reflected from different parts of the membrane as explained in Ref. [18(4)]. It is important to emphasize that during the measurements of optical responses the vortex motion was absent.

The vortices appear only when the amplitude of the acoustic pressure reaches a certain value. In-plane vortex flow was visualized by solidlike islands generated on the film surface, as explained earlier and shown in Fig. 3(a). Analyzing the motion of islands captured by a digital camera we were able to calculate the average angular velocity Ω of tracing particles. Figure 4(b) presents the frequency dependence of this velocity Ω near the resonance frequency $\nu = 350$ Hz. Before disappearing the islands had enough time to make several tens of revolutions. It is clearly shown that the frequency dependence of the angular velocity Ω correlates quite well with the resonance curve of bending modes [see Fig. 4(a)]. This demonstrates that the vortex motion is generated due to transverse oscillations of the smectic film.

Figures 4(c) and 4(d) show the typical trajectory of islands and their velocity on the trajectory, respectively, at an acoustic pressure higher than ~0.16 Pa, when the tracers are not Lagrangian particles as explained earlier. The trajectory of particles was slightly asymmetrical and differs from a circle because of interaction between vortex structures. Each point in the figure was obtained as a result of time averaging over about 10 film oscillations. The time interval between two consecutive shots of CCD camera was 1/30 s, while the period of membrane oscillations was 1/350 s. Figure 4(d) demonstrates the complex motion of islands on a regular trajectory; the membrane center (point C) serves as a stop point, where islands slow down significantly.

Figure 4(e) demonstrates the threshold behavior of the island's velocity vs the amplitude of the acoustic pressure for some particular island. For the indicated pressures islands are distributed on the film surface uniformly (see [18(2)]), and each island has a unique trajectory. We believe that in this case the tracers can be approximately treated as passive particles. The dependence $\Omega(\Delta p)$ has a pronounced yield stress, $\Delta p_0 = 0.063$ Pa, which slightly depends on the concentration of islands. Above threshold the tracked island abruptly begins to move at some finite velocity. This fact reflects the non-Newtonian behavior of smectic crystals

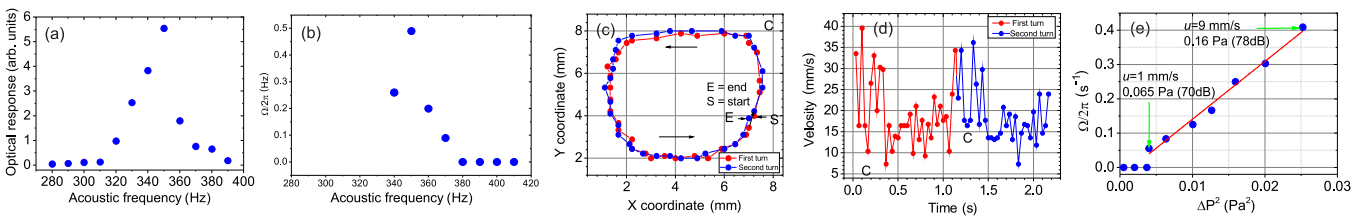

FIG. 4. Experimental results of the acoustic streaming study for a slightly rectangular film: $a = 16.5$ mm, $b = 17$ mm. (a) The size of the laser-beam projection on a screen after reflection from a surface of the film vs the frequency of the acoustic excitation. (b) Angular velocity of islands depending on the acoustic frequency; $\Delta p = 0.2$ Pa. (c) Trajectory of the solidlike island. Point C is the membrane center; $\Delta p = 0.2$ Pa, $\nu = 350$ Hz. (d) The velocity of the island on the trajectory depending on time point C corresponds to the passage of the island near the membrane center; $\Delta p = 0.2$ Pa, $\nu = 350$ Hz. (e) Island angular velocity depending on the squared amplitude of the acoustic pressure; $\nu = 350$ Hz.

belonging to a class of Bingham liquids [13]. In a Bingham liquid when a shear stress is below some threshold value, only elastic behavior is observed. Above threshold one observes an onset of plastic flow. It is well known that in liquid crystal viscoplastic behavior occurs when it contains an elastic lattice, composed of interacted topological defects, e.g., coupled edge dislocations [13,20]. Consequently, the flow is structurally suppressed and the acoustic pressure below threshold provokes only finite deformations of the film. It should be emphasized that in our experiment the motion of islands appears abruptly, whereas in a Bingham body the flow occurs gradually. Evidently, this behavior corresponds to the abrupt destruction of the lattice of topological defects.

Discussion. The theory of 2D vortex motion in acoustically excited, freely suspended smectic films has been developed in Ref. [8]. The key point of this approach was the consideration of two time-shifted degenerate bending modes, excited in the film and coupled by nonlinear interaction. An explicit expression for the vertical vorticity ϖ_z on the film surface in terms of the film displacement was obtained. The main result of the theoretical approach can be written in the form

$$\varpi_z = A(x,y)\Delta p^2 \sin\phi, \tag{3}$$

where the phase shift ϕ describes the time shift between bending modes and $A(x,y)$ characterizes the vorticity spatial distribution. The restoration of vertical vorticity by observation of the motion of passive particles on the film surface is discussed in Ref. [16]. It turns out that the measured vorticity can be described by the same Eq. (3) up to a numerical factor.

Next, we briefly discuss the nature of the phase shift ϕ between excited bending modes. The temporal behavior of the bending mode (n,m) is governed by the equation

$$\left(\partial_t^2 + 2\alpha_{nm}\partial_t + \omega_{nm}^2\right)\xi_{nm} = f_{nm}\cos(\omega t), \tag{4}$$

where ξ_{nm} is the membrane elevation, $\omega_{nm} = 2\pi\nu_{nm}$ is an eigenfrequency, see Eq. (2), α_{nm} characterizes the attenuation of the bending mode [8], f_{nm} is the external force, and ω is its frequency. The forced solution of this equation is

$$\xi_{nm}(t) = \frac{f\cos\left(\omega t + \arctan\left[\frac{2\alpha_{nm}\omega}{\omega_{nm}^2-\omega^2}\right]\right)}{\sqrt{\left(\omega_{nm}^2-\omega^2\right)^2 + 4\alpha_{nm}^2\omega^2}}, \tag{5}$$

and we note that the elevation $\xi_{nm}(t)$ is time-shifted relative to the external force. For a rectangular frame, the eigenmodes (n,m) and (m,n), $n \neq m$, have different eigen frequencies and therefore they are time-shifted relative to each other. For a square frame, $\nu_{nm} = \nu_{mn}$, and the phase shift ϕ is 0.

Experimental results are in good agreement with theoretical predictions. For excited bending modes (3,1) and (1,3) the theory predicts four counter-rotating vortices and we have observed them experimentally [see Fig. 3(b)]. Next, according to the theory the phase shift ϕ should be equal to 0 for the square film and there is no vorticity in that case [see Eq. (3)]. Upon changing the aspect ratio of the frame near that point, $a/b = 1$, we have observed that vortices changed the direction of their rotation as predicted (see [18(5)]). We have also shown that above threshold the angular velocity Ω of the island is proportional to the squared acoustic pressure Δp in accordance with expression (3) [see Fig. 4(e)]. Thus, we have proved experimentally that vortex motion at the film surface is a second-order nonlinear effect.

Highly inhomogeneous acoustic excitation provides even more powerful horizontal streaming control. It allows us to change the spatial distribution of vortices and obtain more intense currents. We propose to use the phenomenon of acoustic streaming for mixing small amounts of matter. The rotational speed of this mixer reaches 600 rpm and the direction of rotation can be tuned by the acoustic frequency. Modulation of the acoustic excitation signal can be used as an additional control parameter. Note that under the same conditions we observed a coalescence effect, which can find applications as a particle manipulation technique. See supplemental videos for illustration [18(6–8)]. We also would like to add that we were unable to get a stable vortex pattern in the case of a too narrow frame, e.g., with a width $b < 5$ mm (see also [21]). The reason for the suppression of vortex motion in the case of small frames probably is the strong influence of the solid boundary including the meniscus, called the "wall" effect in [22]. Much work remains to be done to explain this phenomenon in detail.

It is also necessary to say a few words about the two-dimensionality of freely suspended films. Soap films are not strictly 2D because their in-plane flow is accompanied by a change in film thickness [23]. Nevertheless, these films were considered as model systems providing an opportunity to test 2D turbulence theory. The enstrophy cascade from large scales to small scales was confirmed experimentally on soap films [24]. However, detailed analysis has shown that the fluid motion in soap films is more complex and that the relation to motion described by the 2D hydrodynamic equations is not straightforward [25]. On the other hand, smectic thermotropic films, retaining a constant thickness during the flow, are free of these shortcomings. Let us consider slow motion excited in the smectic film. From the incompressibility condition we obtain that the velocity $\boldsymbol{u}$ is directed in the X-Y film plane, i.e., $u_z \sim ukh \ll u$, where h is the film thickness and $1/k$ is the characteristic scale of horizontal motion, e.g., the size of the vortex. Based on experimental measurements, we can also estimate the variation of the horizontal velocity δu with the film thickness. For highly inhomogeneous acoustic excitation we obtain $\eta\delta u/h \sim \Delta p$, where $\eta = 5\times10^{-2}$ Pa · s is the smectic dynamic viscosity [26] and $\Delta p \sim 0.5$ Pa is the acoustic pressure, and thus $\delta u \sim 2\times 10^{-3}$ mm/s. With the same parameters, the measured horizontal velocity was $u \sim 25$ mm/s, and therefore the velocity field in thin smectic films is two-dimensional with a high accuracy.

In conclusion, we have presented the first-ever experimental observation of acoustic streaming in smectic liquid crystal films. The 2D hydrodynamic flow in the form of vortex couples was studied by observing the motion of disk-shaped islands generated on the film surface. The threshold character of vortex motion was found. We associate the threshold of acoustic streaming with a Bingham-like behavior of the liquid crystal membrane, but the phenomenon requires further investigation. We believe that smectic freely suspended films can be used to study the relationship between the microscopic properties of lamellar materials and their viscoelastic behavior. In addition, we propose the implementation of freely

suspended smectic films for the study of 2D hydrodynamics and in models of large global circulation [27]. Our findings can also be used to provide driving power for microfluidic mixers.

Acknowledgments. We are grateful to V. Lebedev, E. Kats, and S. Vergeles for valuable discussions. This work was supported by the Russian Science Foundation (Project No. 14-12-00475).

[1] D. Vorländer, *Kristallinisch-flüssige substanzen* (Enke, Devon, UK, 1908).
[2] W. T. S. Huck (ed.), *Nanoscale Assembly: Chemical Technique* (Springer-Verlag, Berlin, 2005), p. 123.
[3] IHS Technology, *Polarizer & Optical Films Market Tracker* (IHS Technology, New York, 2015).
[4] H. G. Craighead, J. Cheng, and S. Hackwood, Appl. Phys. Lett. **40**, 22 (1982).
[5] G. H. Brown (ed.), *Advances in Liquid Crystals* (Academic Press, New York, 1976), p. 320.
[6] P. Pieranski, L. Bieliard, J.-Ph. Tournelles, X. Leoncini, C. Furtlehner, H. Dumovlin, E. Rion, B. Jouvin, J.-P. Fenerol, Ph. Palaric, J. Heuving, B. Cartier, and I. Kraus, Physica A **194**, 364 (1993); P. Oswald and P. Pieranski, *Smectic and Columnar Liquid Crystals: Concepts and Physical Properties Illustrated by Experiments* (CRC Press, Boca Raton, FL, 2015).
[7] S. V. Yablonskii, K. Nakano, A. S. Mikhailov, M. Ozaki, and K. Yoshino, Jpn. J. Appl Phys. **42**, 198 (2003); M. J. Golay, Rev. Sci. Instrum. **18**, 357 (1947); S. V. Yablonskii, V. V. Bondarchuk, E. A. Soto-Bustamante, P. N. Romero-Hasler, M. Ozaki, and K. Yoshino, J. Exp. Theor. Phys. **120**, 725 (2015).
[8] V. M. Parfenyev, S. S. Vergeles, and V. V. Lebedev, JETP Lett. **103**, 201 (2016); **104**, 287 (2016).
[9] S. Taylor, Proc. R. Soc. Lond. **27**, 71 (1878).
[10] J. M. Vega, F. J. Higuera, and P. D. Weidman, J. Fluid Mech. **372**, 213 (1998).
[11] S. V. Filatov, V. M. Parfenyev, S. S. Vergeles, M. Yu. Brazhnikov, A. A. Levchenko, and V. V. Lebedev, Phys. Rev. Lett. **116**, 054501 (2016).
[12] A. Pattanaporkratana, C. S. Park, J. E. Maclennan, and N. A. Clark, Ferroelectrics **310**, 131 (2004); P. V. Dolganov, N. S. Shuravin, V. K. Dolganov, and E. I. Kats, JETP Lett. **101**, 453 (2015).
[13] M. P. Mahajan, M. Tsige, P. L. Taylor, and C. Rosenblatt, Liq. Cryst. **26**, 443 (1999); M. Kleman and O. D. Lavrentovich, *Soft Matter Physics* (Springer, Berlin, 2003); Y. Galerne, J. Phys. Lett. **40**, 73 (1979); R. Bartolino and J. Durand, Mol. Cryst. Liq. Cryst. **40**, 117 (1977).
[14] E. B. Sirota, P. S. Pershan, L. B. Sorensen, and J. Collett, Phys. Rev. A **36**, 2890 (1987).
[15] D. Davidov, C. R. Safinya, M. Kaplan, S. S. Dana, R. Schaetzing, R. J. Birgeneau, and J. D. Litster, Phys. Rev. B **19**, 1657 (1979).
[16] V. M. Parfenyev, S. S. Vergeles, and V. V. Lebedev, Phys. Rev. E **94**, 052801 (2016).
[17] J. A. C. Humphrey, J. W. Smith, B. Davey, and R. L. Hummel, Chem. Eng. Sci. **29**, 308 (1974).
[18] See Supplemental Material at http://link.aps.org/supplemental/10.1103/PhysRevE.95.012707: 1, visualization of in-plane flow by disk-shaped islands; 2, behavior of islands at different acoustic pressures; 3, visualization of in-plane flow by an excess number of islands; 4, detection method of mode indices by the optical pattern analysis; 5, influence of the film geometry on acoustic streaming; 6, changing the direction of rotation by the acoustic frequency; 7, acoustic streaming under a modulated excitation signal; 8, coalescence effect.
[19] V. O. Afenchenko, A. B. Ezersky, S. V. Kiyashko, M. I. Rabinovich, and P. D. Weidman, Phys. Fluids **10**, 390 (1998).
[20] S. Fujii, S. Komura, Y. Ishii and C-Y. D. Lu, J. Phys.: Condens. Matter **23**, 235105 (2011).
[21] M. Brazovskaia, H. Dumoulin, and P. Pieranski, Phys. Rev. Lett. **76**, 1655 (1996); S. Uto, E. Tazoh, M. Ozaki, and K. Yoshino, J. Appl. Phys. **82**, 2791 (1997).
[22] Z. Qi, C. S. Park, M. A. Glaser, J. E. Maclennan, and N. A. Clark, Phys. Rev. E **93**, 012706 (2016).
[23] S. D. Danilov and D. Gurarie, Usp. Fiz. Nauk **170**, 921 (2000).
[24] H. Kellay, X. L. Wu, and W. I. Goldburg, Phys. Rev. Lett. **80**, 277 (1998).
[25] Y. Couder, J. M. Chomaz, and M. Rabaud, Physica D **37**, 384 (1989).
[26] F. Schneider, Phys. Rev. E **74**, 021709 (2006).
[27] F. Seychelles, Y. Amarouchene, M. Bessafi, and H. Kellay, Phys. Rev. Lett. **100**, 144501 (2008).